Spatial and temporal diversity of glycome expression in mammalian brain

Jua Lee[a,b], Seungshin Ha[c], Minsoo Kim[c], Seong-Wook Kim[c], Jaekyung Yun[a,b], Sureyya Ozcan[d,e], Heeyoun Hwang[f], In Jung Ji[a,b], Dongtan Yin[a,b], Maree J. Webster[g], Cynthia Shannon Weickert[h,i,j], Jae-Han Kim[k], Jong Shin Yoo[a,f], Rudolf Grimm[a,l], Sabine Bahn[d], Hee-Sup Shin[c,1,2], and Hyun Joo An[a,b,1,2]

[a]Graduate School of Analytical Science & Technology, Chungnam National University, 34134 Daejeon, South Korea; [b]Asia-Pacific Glycomics Reference Site, 34134 Daejeon, South Korea; [c]Center for Cognition and Sociality, Institute for Basic Science, 34051 Daejeon, South Korea; [d]Department of Chemical Engineering and Biotechnology, University of Cambridge, CB2 1QT Cambridge, United Kingdom; [e]Department of Chemistry, Middle East Technical University, 06800 Ankara, Turkey; [f]Research Center for Bioconvergence Analysis, Korea Basic Science Institute, 28119 Cheongju, South Korea; [g]Laboratory of Brain Research, The Stanley Medical Research Institute, Chevy Chase, MD 20815; [h]Schizophrenia Research Laboratory, Neuroscience Research Australia, Randwick, NSW 2031, Australia; [i]School of Psychiatry, University of New South Wales, Sydney, NSW 2052, Australia; [j]Department of Neuroscience & Physiology, Upstate Medical University, Syracuse, NY 13210; [k]Department of Food and Nutrition, Chungnam National University, 34134 Daejeon, South Korea; and [l]Agilent Technologies Inc., Santa Clara, CA 95051

Contributed by Hee-Sup Shin, October 5, 2020 (sent for review July 9, 2020; reviewed by Carlito B. Lebrilla, David M. Lubman, Alcino J. Silva, and Jeongmin Song)

Mammalian brain glycome remains a relatively poorly understood area compared to other large-scale "omics" studies, such as genomics and transcriptomics due to the inherent complexity and heterogeneity of glycan structure and properties. Here, we first performed spatial and temporal analysis of glycome expression patterns in the mammalian brain using a cutting-edge experimental tool based on liquid chromatography-mass spectrometry, with the ultimate aim to yield valuable implications on molecular events regarding brain functions and development. We observed an apparent diversity in the glycome expression patterns, which is spatially well-preserved among nine different brain regions in mouse. Next, we explored whether the glycome expression pattern changes temporally during postnatal brain development by examining the prefrontal cortex (PFC) at different time point across six postnatal stages in mouse. We found that glycan expression profiles were dynamically regulated during postnatal developments. A similar result was obtained in PFC samples from humans ranging in age from 39 d to 49 y. Novel glycans unique to the brain were also identified. Interestingly, changes primarily attributed to sialylated and fucosylated glycans were extensively observed during PFC development. Finally, based on the vast heterogeneity of glycans, we constructed a core glyco-synthesis map to delineate the glycosylation pathway responsible for the glycan diversity during the PFC development. Our findings reveal high levels of diversity in a glycosylation program underlying brain region specificity and age dependency, and may lead to new studies exploring the role of glycans in spatiotemporally diverse brain functions.

mammalian | brain | spatiotemporal | glycosylation | LC-MS

The complexity of molecular mechanisms involved in mammalian brain region specificity and development has begun to emerge thanks to recent advances in "omics" technologies. Simultaneous monitoring of vast numbers of molecules in the distinct subregions (1–4) and developmental stages of brain (5–8) have facilitated the mapping of the genome, transcriptome, proteome, and metabolome in animals as well as human. Glycosylation, one of the most common posttranslational modifications of proteins (9), has long attracted considerable attention because of its tremendous level of complexity, and therefore potentially important roles in the central nervous system (10), especially in region-specific regulation (11), development (12), and differentiation (13, 14). Recent studies indicated that profiles of the neuronal genome, transcriptome, and proteome were tightly linked to the glycome (15). However, to our knowledge, comprehensive glycome studies for investigating the spatiotemporal diversities of glycan in the brains of human and animals have not been reported due to the limited availability of samples and the lack of appropriate analytical tools for probing structures and properties of the glycome (16). For the same reason, most brain glycosylation studies have focused on the cellular level and target proteins in specific cell-types, not in subregions of the brain.

Every eukaryotic cell in nature is surrounded by a rich surface coat composed of glycolipids and glycoproteins, termed the glycocalyx, which forms the interface between the cell and its outside world and acts as a mediator and transducer of environmental information to the cell (9). In particular, glycans play a pivotal role in various functions depending on neural cell interactions such as neurite outgrowth and fasciculation, synapse formation and maturation, and modulation of synaptic transmission and plasticity (12). Recently, it has been reported that glycosylation presents an incredible level of structural diversity according to different biosystems, ranging from species-specificity (17) to organ-specificity (11), that is further extended by micro- and macroheterogeneity. In particular, anatomical and cell differentiation studies have shown that glycosylation in brain function may be spatially and temporally relevant in

Significance

Deciphering molecular mechanisms at the glycome level in mammalian brain remains a missing piece of the puzzle in molecular neuroscience due to the intrinsic complexity of glycosylation and the lack of analytical tools. Here, we uncovered the variation and diversity of glycome expression in human and mouse brain samples according to spatial and temporal differences. We further constructed a comprehensive synthesis map using glycans structurally elucidated by LC-MS/MS and found strong evidence on the conservation and developmental divergence of human and mouse prefrontal cortex N-glycome. Our data could be the reference for future mammalian brain glycome study. Furthermore, it provides valuable information on human brain glycome, which has languished in relative obscurity.

Author contributions: M.J.W., C.S.W., R.G., S.B., H.-S.S., and H.J.A. designed research; J.L., S.H., M.K., S.-W.K., J.Y., S.O., H.H., I.J.J., D.Y., M.J.W., C.S.W., J.-H.K., J.S.Y., R.G., and S.B. performed research; J.L. and H.J.A. analyzed data; and J.L., H.-S.S., and H.J.A. wrote the paper.

Reviewers: C.B.L., University of California, Davis; D.M.L., University of Michigan; A.J.S., University of California, Los Angeles; and J.S., Cornell University.

Competing interest statement: H.J.A. and Carlito B. Lebrilla are coauthors on a 2019 method article.

See online for related content such as Commentaries.

[1]H.-S.S. and H.J.A. contributed equally to this work.

[2]To whom correspondence may be addressed. Email: shin@ibs.re.kr or hjan@cnu.ac.kr.

This article contains supporting information online at https://www.pnas.org/lookup/suppl/doi:10.1073/pnas.2014207117/-/DCSupplemental.

First published November 2, 2020.

mammalian, but do not provide sufficient information on the diversity and complexity of glycosylation. The challenge arises from the structural and quantitative profile of glycosylation from brain matrices. Glycans are inherently unpredictable because they are synthesized stepwise in a nontemplate-driven manner by numerous glycosyltransferases that are in competition with each other, unlike nucleic acids or proteins that are synthesized in a template-driven manner (18). In addition, only a small fraction of the protein glycosylation repertoire can be decoded depending on genomic DNA sequences since glycosylation is highly influenced by the physiological status of cells (19). Particularly, determining brain glycosylation is analytically challenging because the amount of carbohydrates in the brain is very small compared with other major components, such as fat. Highly sensitive analytical tools spanning the range from glycan extraction to glycan detection are required to comprehensively probe heterogeneous glycans bound to proteins in the brain. Liquid chromatography coupled with mass spectrometry (LC-MS) providing a systems-level view has recently emerged as a powerful technique for examining the glycome in mammalian tissues (20, 21). However, this approach has not yet been extensively applied to the study of brain glycosylation. Comprehensive profile and comparative characterization of the mammalian brain glycome have remained missing pieces of the molecular-components puzzle in neuroscience. Thus, there is no doubt that elucidating complex brain glycan structures would be an important first step toward understanding the relationship between spatiotemporal dynamics in glycan phenotype and biological functions.

Until now, investigations of protein-bound N-glycans, the "true glycome" constituting the largest portion of glycosylation, have not received attention as brain glycome studies focused instead on oligomeric glycosylation (e.g., neural cell adhesion molecules). In a previous study, we established a powerful, highly sensitive, and reproducible analytical platform for qualitative and quantitative exploration of the brain glycome, which is comprehensive tissue glyco-capture with porous graphitized carbon (PGC) nano-LC/MS (22). In this study, in order to understand relationship between spatiotemporal alteration of the brain and glycosylation, we performed a systematic, in-depth N-glycan analysis of the human and mouse brain using PGC nano-LC/MS/MS. Regional distribution of glycans was examined for nine mouse brain regions (cerebral cortex, prefrontal cortex, striatum, hippocampus, olfactory bulb, diencephalon, midbrain, pons-medulla, cerebellum). We next targeted the prefrontal cortex (PFC) region, which is particularly vulnerable to lesions because of its protracted developmental process for examining temporal variation in glycomic signatures and their relationships to mammalian PFC development. In human, altered structure and gross morphology in the PFC have been observed during brain development (23). Furthermore, diverse functions of the brain (e.g., cognition, emotion, sociability, and so forth) are dependent on this brain area.

For these reasons, the PFC region in the brain has been considered as a critical area for brain development (23). In particular, unique characteristics in phylogeny, as well as ontogeny, were detected in the human PFC (24). The size of the PFC relative to the whole brain has increased with mammalian evolutionary progression, reaching its maximum relative size in humans (24). According to most indices of development, the PFC is also one of the last cortical regions to keep on maturing during the course of individual development. However, despite the important roles of the PFC in the brain, the molecular mechanisms in the PFC underlying development, particularly in relation to glycosylation, remain largely unknown. Here, we obtained age-related glycan profiles from 30 mouse PFC samples covering 6 comparable developmental time periods (1, 2, 3, 6, 10, and 43 wk) and 68 human PFC samples covering 7 developmental time frames (neonate, infant, toddler, school age, teenager, young adult, and adult). We successfully identified and quantified 142 and 136 N-glycans containing brain-unique moieties, such as sialylated *N*,*N*-diacetyl lactosediamines (sialylated GalNAc-GlcNAc, sialylated LacdiNAc) LacdiNAc in extracts of human and mouse brain samples, respectively. Glycans containing similar structural traits, including sialylated LacdiNAc and Lewis Y(B) epitope, readily showed region-specificity. In addition, we observed that several glycan groups with mainly sialic acid and fucose residues were significantly altered during PFC development in mouse and human. Finally, we constructed a PFC N-glycome synthetic map to pinpoint developmental stage-specific pathways and provide an overall picture of the diversity of glycan expression. Our study demonstrates spatiotemporal divergence of glycome patterns in the brain across the entire cellular milieu that transcend cellular- or target protein-level resolution.

Results

To examine neuronal glycome diversity according to brain regions and ages, we prepared 9 mice brain region samples from 5 adult male mice (Fig. 1*A*), 68 human PFC samples covering 7 developmental time frames, and mouse PFC samples covering 6 comparable developmental time periods from 5 mice per age group (Fig. 1*B*). A streamlined workflow for the study of brain glycosylation is illustrated in Fig. 1*C*. See *SI Appendix*, *Supplementary Methods* for detailed information.

Spatial Diversity of Glycan Expression in Mouse Brain. A total of 130 glycans were found in mouse brain samples across all brain regions (refer to *SI Appendix*, Table S1 for the full list of glycans and their abundances). To obtain a comprehensive overview of glycan profiles, we plotted each glycan composition against its frequency (occurrence) of detection (Fig. 2*A*). Forty-four glycans, accounting for 90% (normalized absolute peak intensity, NAPI) of total glycans, were detected in all mouse brain region samples. These glycans were mainly high-mannose (HM) and complex-hybrid types consisting of Hexose (Hex) and *N*-acetyl hexosamine (HexNAc) in combination with fucose (Fuc), and sialic acid residues such as *N*-acetylneuraminic acid (NeuAc) and Hexuronic acid (HexA). The presence of highly abundant fucosylated glycans has been recognized as one of the unique glycomic characteristics of the brain compared with other tissues and body fluids (20, 22). Indeed, we observed highly fucosylated glycans containing $[Fuc]_{1-5}$ in all mouse brain regions.

Univariate analysis performed by one-way ANOVA yielded 87 altered glycan species when comparing all brain region groups (*SI Appendix*, Fig. S1). With these altered glycans, multivariate analysis was performed by sparse partial least-squares discriminant analysis (sPLS-DA) (Fig. 2*B*). Generally, the score plot of the sPLS-DA showed a relatively clear segregation of experimental groups according to regions (component 1 = 24.6% and component 2 = 13.3%), even though the cerebellum group showed considerable overlap with hippocampus, olfactory bulb, pons-medulla. In addition, we validated the clusters from the sPLS-DA using area under the receiver operating characteristic curve (AUC-ROC) (*SI Appendix*, Fig. S2). As shown in Fig. 2*B*, the cerebellum group showed considerable overlap with the hippocampus, olfactory bulb, pons-medulla in the component 1 and 2 from sPLS-DA. From the AUC-ROC curve tested with a specific region vs. others, we found low AUC values (<0.90) from the cerebellum, hippocampus, olfactory bulb, and pons-medulla. In contrast, very high AUC values (>0.95) were observed in the cerebral cortex, PFC, diencephalon, and striatum, where they are relatively well-clustered in each region. Then we selected the specific glycans which are most strongly associated with regional distribution in order to assess variation of glycans according to brain regions (variable importance in the projection score of glycan profile was shown in *SI Appendix*, Table S2). The segregation trend was associated with high levels of $Hex_5HexNAc_4$, $Hex_4HexNAc_4$, $Hex_3HexNAc_6Fuc_1$ observed in the PFC,

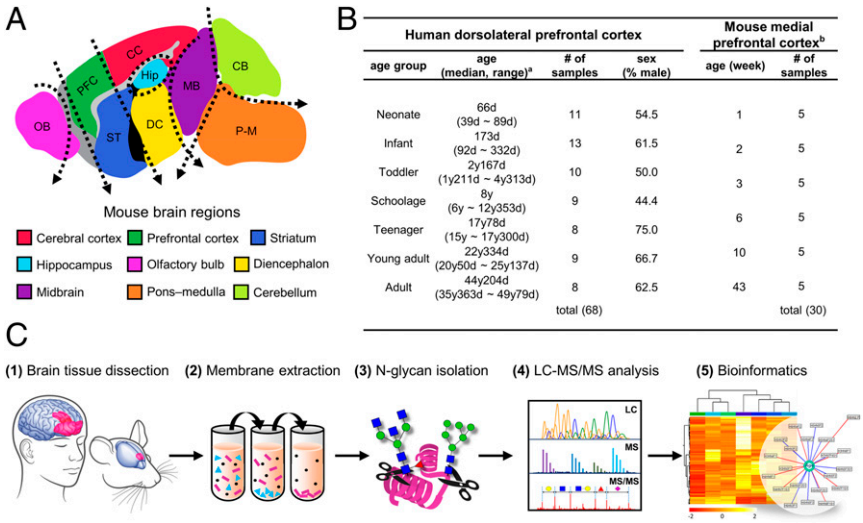

B

Human dorsolateral prefrontal cortex				Mouse medial prefrontal cortex[b]	
age group	age (median, range)[a]	# of samples	sex (% male)	age (week)	# of samples
Neonate	66d (39d ~ 89d)	11	54.5	1	5
Infant	173d (92d ~ 332d)	13	61.5	2	5
Toddler	2y167d (1y211d ~ 4y313d)	10	50.0	3	5
Schoolage	8y (6y ~ 12y353d)	9	44.4	6	5
Teenager	17y78d (15y ~ 17y300d)	8	75.0	10	5
Young adult	22y334d (20y50d ~ 25y137d)	9	66.7	43	5
Adult	44y204d (35y363d ~ 49y79d)	8	62.5		
		total (68)			total (30)

Fig. 1. Experimental outline of glycomic profiling of the human and mouse brains. (*A*) Information on mouse brain regions. CB, cerebellum; CC, cerebral cortex; DC, diencephalon; Hip, hippocampus; MB, midbrain; OB, olfactory bulb; PFC, prefrontal cortex; P-M, pons-medulla; ST, striatum. (*B*) Information on human dorsolateral PFC and mouse medial PFC samples, respectively. [a]y and d represent years and days, respectively; [b]male mouse samples collected. (*C*) Illustration of the experimental workflow.

olfactory bulb, and cerebellum, and low levels of $Hex_5HexNAc_5Fuc_3$, $Hex_6HexNAc_5Fuc_3NeuAc_1$, $Hex_5HexNAc_4Fuc_3$, $Hex_4HexNAc_4Fuc_2$, $Hex_4HexNAc_3Fuc_2$, $Hex_5HexNAc_5Fuc_2$, and $Hex_6HexNAc_4Fuc_3$ observed in the PFC, hippocampus, olfactory bulb, and cerebellum as revealed by the top 10 loading 1 values (Fig. 2*C*).

On the other hand, high levels of several glycans observed in the cerebral cortex compared to other regions were related to separating groups from other regional groups, as indicated by the top 10 loading 2 values (Fig. 2*D*). A cluster of the cerebral cortex was successfully distinguished from other groups such as midbrain, diencephalon, and striatum by variance of the second component. Most of glycans of loading 2 showed relatively high intensity in the cerebral cortex, which ensured clustering between the areas.

Furthermore, 87 altered glycans were plotted as clusters in the heat map plot (Fig. 2*E*) in order to gain broad understanding of the glycomic variation and similarity level between individual samples. Note that most of the samples from each region were clustered together, except for one striatum sample. Interestingly, biosynthetically relevant glycan compositions were divided into seven cluster groups. In particular, several glycan groups with similar structural properties, such as fucosylated glycans with sialylated HexNAc, hybrid type with bisection, sialylated hybrid type, sialylated LacdiNAc, sialylated HexNAc, highly branched and highly fucosylated, and Lewis Y(B) are found in each cluster. Representative putative glycan structures of each cluster are shown in *SI Appendix*, Fig. S3. For example, cluster 5 contains sialylated LacdiNAc, while the sialylated hybrid type appear in cluster 3. Other glycans with high structural similarity in each cluster are highlighted in the sugar code in Fig. 2*E*.

Temporal Diversity of Glycan Expression in Mammalian PFC. We next analyzed the PFC, which undergoes a prolonged course of maturation with variations in its fine structure and gross morphology as a function of age for examination of temporal diversity of glycome profiling. A total of 142 and 136 glycans were found in human and mouse PFC samples, respectively, across all age groups (refer to *SI Appendix*, Table S3 for the full list of glycans and their abundances). *SI Appendix*, Fig. S4 shows identified glycan compositions and their frequency (occurrence) of detection in all human PFC samples and mouse PFC samples, respectively. All 136 glycans observed in mouse PFCs were detected in human PFCs. Five minor glycans accounting for 0.13% (average sum of NAPI), including highly branched and fucosylated glycans and fucosylated glycans containing HNK-1 [HSO_3-GlcA–Gal–GlcNAc], were observed only in human (*SI Appendix*, Table S3, see glycan compositions marked by underlining). Fifty-two glycans accounting for 77% (NAPI) of total glycans were detected in all human PFC samples regardless of age status or individual variation (*SI Appendix*, Fig. S4*A*). In the mouse PFC, 59 glycans accounting for 73% (NAPI) of total glycans were found in all samples (*SI Appendix*, Fig. S4*B*). Of these glycans, 44 were observed in both species, strongly suggesting that major (basic) N-glycosylation is highly conserved between two species. Interestingly, glycosylation was highly conserved between humans and mice, but the proportion of glycans with a frequency less than 50% of total glycans was 1.4-fold higher in humans than in mice, indicating that human PFC glycans exhibit slightly higher individual variation than mouse PFC glycans.

A heat map hierarchical cluster presentation of the abundances of mouse PFC N-glycans was generated to visualize changes in glycosylation during PFC development and to determine the relationship between the age groups (Fig. 3*A*). The heat map cluster dendrograms showed a clear division into a younger cluster (1-, 2-, and 3-wk-old) and an older cluster (6-, 10-, and 43-wk-old). The greatest change in glycosylation was observed between 3-wk-old (corresponding to the human toddler period) and 6-wk-old (corresponding to the human teenager period), which eventually led to their separation into two different clusters. Interestingly, human PFC tissues also showed changes in glycosylation during development. (Fig. 3*B*). As in the case of mouse PFCs, the resulting dendrograms revealed that the seven age groups could be clearly divided into two clusters: A younger cluster (neonate, infant, toddler, and school age) and an older cluster (teenager, young adult, and adult). In general, adjacent developmental stages were closely connected to each other. Interestingly, the greatest change in glycosylation was observed between school-age and teenager groups, which were separated into different clusters. Note that the greatest heterogeneity in mouse PFC glycosylation occurred between 3- and 6-wk-old mouse ages, equivalent to those in human based on previously reported developmental milestones (25). The neonate group, the youngest age group, is clustered with the

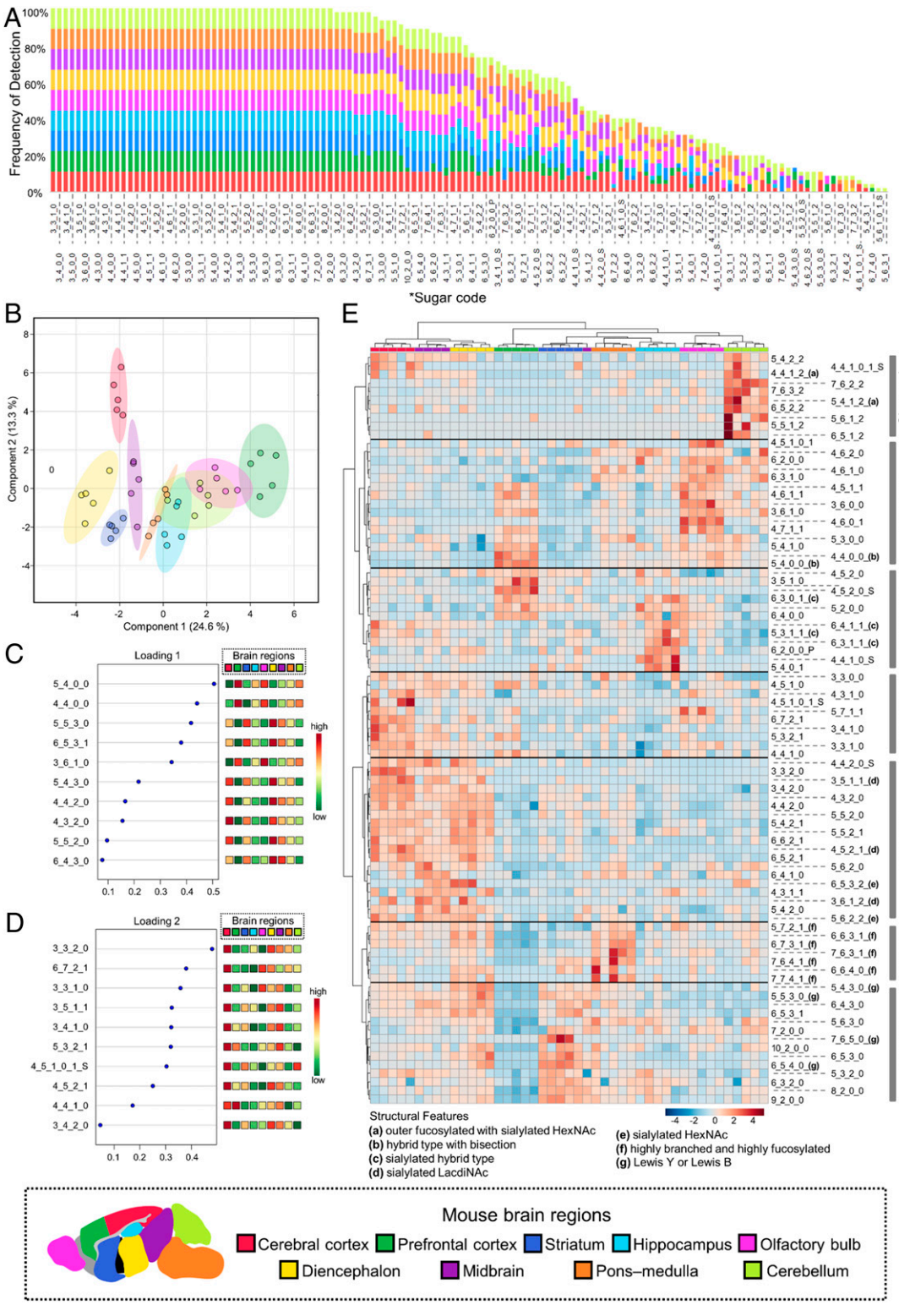

Fig. 2. Regional comparison based on glycan expression in mouse brain. *Sugar code: Hex_HexNAc_Fuc_NeuAc_(HexA)_phosphorylation (P) or sulfation (S). (*A*) Frequency of detection of nine mouse brain N-glycan compositions in mass profiles. (*B*) sPLS-DA score plots of mouse brain samples between nine brain regions. (*C* and *D*) Top 10 glycan species according to loading 1 values and loading 2 values of the sPLS-DA, respectively. The variables are ranked by the absolute values of their loadings. (*E*) Heat map for the hierarchical clustering of N-glycans for nine mouse brain regions from five mice. Scale bar indicates *z*-scores of standardized glycan values, with highly expressed glycan depicted in red and low-expressed glycans depicted in blue. Rows correspond to clusters obtained from 87 glycans which are significantly different according to brain regions ($P < 0.01$, ANOVA).

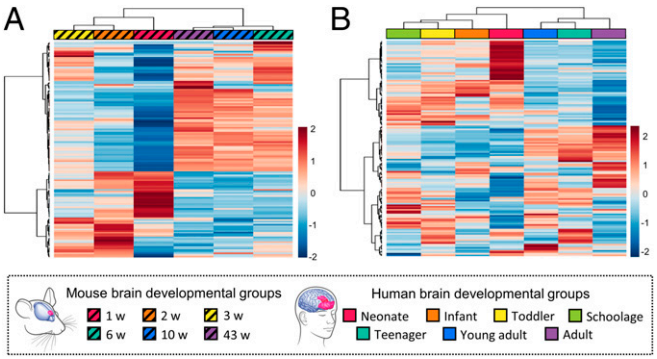

Fig. 3. Relationship between mouse and human PFC samples at different ages according to glycan expression. (*A* and *B*) Heat maps for the hierarchical clustering of PFC N-glycans of six age groups of mice and seven age groups of humans, respectively. Scale bar indicates *z*-scores of standardized glycan values, with highly expressed glycan depicted in red and low-expressed glycans depicted in blue. Rows correspond to clusters obtained from a total of 142 human PFC N-glycans and 136 mouse PFC N-glycans, respectively.

younger group (infant, toddler, and school age), but has more heterogeneous glycosylation than other young groups.

Furthermore, 24 and 36 glycans were found to be significantly changed between younger and older clusters in human and mouse, respectively, by volcano plot (*SI Appendix*, Fig. S5 *A* and *B*). The glycans consist of various glycan species, including mono-, bi-, tri-, and tetra-antennary glycans with $[Fuc]_{0–4}$ and $[NeuAc]_{0–2}$. Among them, five glycans shown in *SI Appendix*, Fig. S5*C* had positive or negative correlations with aging in both human and mouse. In particular, the glycans HNK-1–containing motif seems to be closely associated with entire age range of humans and the younger age in mice (see the glycans marked with asterisks in *SI Appendix*, Fig. S5 *A* and *B*). In addition, we found several interesting structural characters in each younger and older cluster of human and mouse, respectively. Specifically, fucosylated glycans containing sialyled LacdiNAc were found in a younger cluster ($Hex_3HexNAc_6Fuc_1NeuAc_2$ and $Hex_4HexNAc_5Fuc_2NeuAc_1$), while phosphorylated $Hex_6HexNAc_2$ was found in an older cluster in human PFC. On the other hand, sulfated and fucosylated glycan was identified in younger cluster (HSO_3-$Hex_4HexNAc_5Fuc_2$), while sialylated HexNAc ($Hex_6HexNAc_5Fuc_3NeuAc_2$ and $Hex_7HexNAc_6Fuc_4NeuAc_2$), fucosylated glycans containing sialyled LacdiNAc ($Hex_4HexNAc_5Fuc_1NeuAc_2$), and sulfated and fucosylated glycan (HSO_3-$Hex_5HexNAc_5Fuc_3$) were detected in an older cluster in mouse PFC. We also performed a sPLS analysis to examine whether other biological parameters, namely pH, postmortem interval, sex, race, or cause of death, were associated with human PFC glycans in our sample set (*SI Appendix*, Fig. S6 and Table S4). We found that PFC glycans were most closely related to age among numerical variables (age, pH, postmortem interval, and sex) through relevance networks using sPLS (*SI Appendix*, Fig. S6*A*). Additionally, sPLS-DA showed that there were no clusters that showed significant discriminations according to categorical variables (sex, race, and cause of death) (*SI Appendix*, Fig. S6 *B*, *C*, and *D*, respectively). Collectively, these observations represent that the changes in human PFC glycans in a given dataset are largely attributable to biological factors related to age.

Quantitative Changes in Glycosylation during Human PFC Development. For an in-depth characterization of the biological relevance of development-specific glycans, 48 statistically significant human PFC glycans ($P < 0.01$, ANOVA) (*SI Appendix*, Fig. S7*A*) were further investigated using Pearson's correlation. As shown in Fig. 4, human PFC glycans were separated into two main clusters depending on their relevance to age status. Cluster I contained glycans negatively associated with aging, whereas glycans in cluster II had a positive correlation with aging. In addition, the two main clusters (cluster I and II) had distinct subclusters that were closely linked to the glycosynthetic context, reflecting the addition or deletion of monosaccharides (Fig. 4, see asterisk on *y* axis). Highly branched (tri- and tetra-antennary) glycans with high levels of fucose and sialic acid, and glycans containing sialylated LacdiNAc, sialylated HexNAc, and HNK-1 motifs, were found only in cluster I, while bisecting with core fucosylation and phosphorylated HM-type glycans were found only in cluster II. On the other hand, hybrid and Lewis-type glycans, such as LeX(a), sLeX(a), and LeY(b), were found in both clusters.

Interestingly, several glycan types containing unique structural moieties were found to be positively or negatively associated with human PFC development. For example, we found that three sialylated LacdiNAc N-glycans bearing a [NeuAc-HexNAc-HexNAc] residue at the terminal were significantly decreased during development (*SI Appendix*, Table S3, see glycans marked by two asterisks). Genetically, the biosynthesis of LacdiNAc can be mediated by β4GalNAc-T4, one of the β1-4-*N*-acetylgalactosaminyltransferases in the human brain (26), although an association of LacdiNAc-related glycans with the developing human brain has not yet been demonstrated. However, recent studies have indicated that glycans containing LacdiNAc-related epitopes are associated with several biological functions, including malignancy in several types of tumors (27, 28), half-life of circulating pituitary glycohormone (29), self-renewal of mouse embryonic stem cells (30), and differentiation of bovine mammary epithelial cells (31). We also identified nine N-glycans containing the sialylated HexNAc moiety [NeuAc-HexNAc] with at least one fucose residue in the human PFC (*SI Appendix*, Table S3, marked by an asterisk). Interestingly, Torii et al. (32), reported significant variation in 6-sialyl Lewis C, a sialylated HexNAc structure, in developing mouse cerebral cortices. Finally, sulfated complex/hybrid-type glycans corresponding to [HSO_3-$Hex_4HexNAc_5Fuc_2$], [HSO_3-$Hex_5HexNAc_5Fuc_2$], and [HSO_3-$Hex_5HexNAc_5Fuc_2HexA_1$] showed a pattern of decreasing abundance during PFC development.

In addition to glycan groups that are closely related to each other in a biosynthetic context, we observed interesting glycan compounds that were closely associated with PFC development. The first of these was the glycan [HSO_3-$Hex_5HexNAc_5Fuc_2HexA_1$] containing an HNK-1 epitope, which decreased during PFC development. Several studies have previously reported that the HNK-1 epitope is distinctively expressed on several cell adhesion and extracellular matrix proteins (33) and is correlated with neural development (34), as well as learning and neural plasticity (35) (three in mice). We also found that the phosphorylated HM glycan [HPO_3-$Hex_6HexNAc_2$] associated with a specialized trafficking pathway of lysosomes (18) sharply increased during development. Although several research groups have emphasized the association of glycan epitopes with various biological processes, the function of individual glycans in relation to brain development is currently not fully understood. Interestingly, glycans containing unique epitopes as well as known epitopes with increased or decreased expression during human PFC development have been found. These findings provide a valuable resource to guide future follow-up studies targeting development-specific glycans.

Conserved Brain-Specific Glycosylation Patterns in Human and Mouse PFCs. Most studies of brain development have employed rodent models, but the comparability of human and rodent brain development is still unclear (36). To examine similarities and differences in glycosylation between humans and mice, we comprehensively profiled N-glycans extracted from the human brain (PFC), mouse brain (PFC), human serum, and mouse serum using a single analytical platform. Fig. 5 *A* and *B* show the representative total compound chromatograms of serum and brain glycans, respectively. In chromatographic separations on a PGC column, smaller

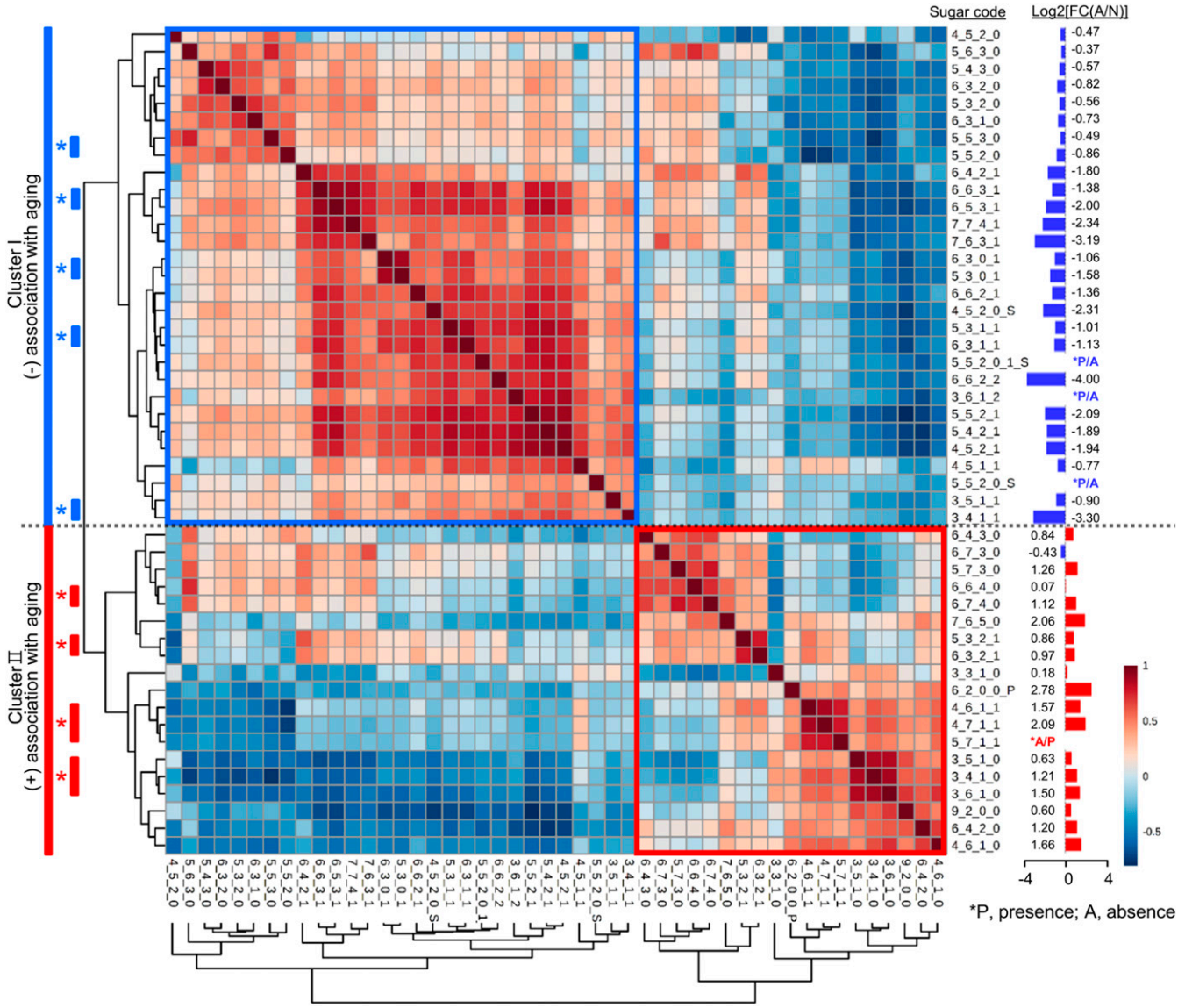

Fig. 4. Characterization of differentially expressed glycans across human PFC development. Heat map showing pairwise correlations of 48 human PFC N-glycans ($P < 0.01$). Glycans with positive and negative associations with aging are indicated with red and blue, respectively. Asterisks show the glycans that were closely linked to the glyco-synthetic context. Bars on the right sides of the heat map show the calculated values of $\log_2$ (fold-change [average of NAPI in adult group/average of NAPI in neonate group]).

(simpler) and neutral glycans elute earlier, whereas larger (more complex) and acidic glycans elute later. Elution behavior in chromatograms of brain samples from mice and humans was very similar, but was highly different between species in serum. We found that the striking difference in glycosylation between serum and brain was predominantly driven by the abundance of acidic glycans, including NeuAc and N-glycolylneuraminic acid (NeuGc), which eluted late. This observation was consistent with previous reports on analysis of mouse serum and brain glycome (22, 37). A statistical analysis of glycans clearly revealed a high correlation between human and mouse brains, but showed little correlation among other samples, indicating that interspecies variation in brain glycosylation was much smaller than intraspecies variation between brain and serum glycosylation (Fig. 5*C*). The weak correlation between species of serum glycans was largely attributable to the presence of the nonhuman sialic acid, NeuGc, only in mouse serum, reflecting the absence of CMP–Neu5Ac hydroxylase (CMAH) in humans (18). Indeed, we did not find NeuGc- or NeuGc-related compounds in human serum. Interestingly, NeuGc-related compounds were not observed in mouse PFCs (Fig. 5*B*). This observation is consistent with a previous report that suppression of NeuGc expression in the brain is universal among all vertebrates tested to date; this contrasts with variable expression of NeuGc in other organs, reflecting differential regulation of CMAH, as exemplified by major expression of NeuGc in mouse liver (38).

To examine similarities and differences in glycosylation in the human brain, mouse brain, human serum, and mouse serum, we performed quantitative comparisons by classifying glycans into five typical classes: High-mannose (HM), complex or hybrid (C/H), complex/hybrid-fucosylated (C/H-F), complex/hybrid-sialylated (C/H-S), and complex/hybrid-fucosylated and sialylated (C/H-FS) (Fig. 5*D*). In both species, C/H-F was the most abundant glycan class in the brain, whereas C/H-S was the most abundant glycan class in serum. Interestingly, the highest abundance of fucosylated glycans was observed in every nine mouse brain regions, as we reported on the hippocampus and the coronal sections of mouse brain in a previous study based on the identical

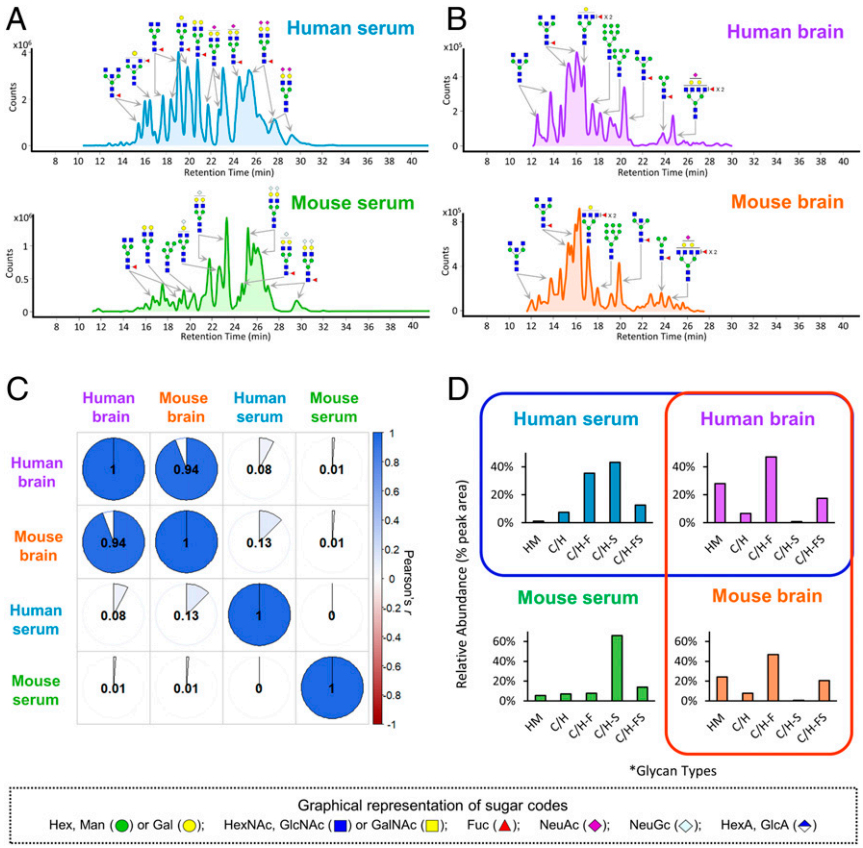

Fig. 5. Comparison of N-glycans found in the brain and serum of humans and mice. (*A* and *B*) Representative total compound chromatograms of N-glycans from *A* human serum (*Upper*) and mouse serum (*Lower*) and (*B*) human PFC (adult, *Upper*) and mouse PFC (43 wk, *Lower*). Representative glycan structures were assigned to each peak. Glycan schematic symbols: yellow circle, galactose; blue circle, glucose; green circle, mannose; blue square, N-acetyl glucosamine; red triangle, fucose; purple diamond, NeuAc; and light gray diamond, NeuGc. (*C*) Pearson correlation analyses using NAPI values of N-glycans from human serum, mouse serum, human brain, and mouse brain samples. Average glycan NAPI values of all 68 human PFCs and 30 mouse PFCs were used for calculation, respectively. Absolute values of Pearson correlation coefficient (*r*) are represented as pie slices of proportional sizes. Scale bar indicates Pearson's *r* from dark red (−1) to dark blue (+1). (*D*) Bar graphs of glycan biosynthetic types in human serum, mouse serum, human brain and mouse brain samples. Average glycan NAPIs of all 68 human PFCs and 30 mouse PFCs were shown as representative values, respectively. *Glycan types: HM, high-mannose; C/H, complex/hybrid; C/H-F, fucosylated complex/hybrid; C/H-S, sialylated complex/hybrid; C/H-FS, fucosylated and sialylated complex/hybrid.

method employed in this study (22). Quantification of patterns based on glycan classes revealed a high similarity between human and mouse brain, while showing substantial differences between human and mouse serum. Nonetheless, brain glycosylation was still clearly distinct from that in serum regardless of species-specific differences, with three glycan classes—C/H-F, C/H-S, and HM—distinguishing brain glycosylation from serum glycosylation. Higher levels of fucosylation, especially trifucosylation, and lower levels of sialylation were observed in brain compared with serum, an observation consistent with a previous report (39). Specifically, incompletely processed asialo- or asialo-agalacto structures were observed in biantennary glycans, which are a major branching type of brain glycosylation, whereas sialylated structures were preferentially observed in higher branched N-glycans (≥triantennary), which are a minor branching type of brain glycosylation. Interestingly, another feature of brain glycosylation observed in both species is a high content of HM glycans, which are involved in the early biosynthesis process, compared with serum. Brain tissue is known to carry HM-type glycans in cell surface-recognition molecules, such as L1, neural cell adhesion molecule, and adhesion molecule on glia, whereas most tissues do not carry oligomannosides at the cell surface because of elimination during the biosynthetic process, which yields mature N-glycans (12).

Comparison of PFC Glycosylation between Humans and Mice during Development. Monitoring changes in glycans during brain development in both humans and mice may provide valuable insights into the characteristics of glycans that are tightly linked with brain development, regardless of species. Thus, we selected 30 glycans that were overlapped between statistically important 48 glycans and 90 glycans in the human PFC and mouse PFC, respectively ($P < 0.01$) (*SI Appendix*, Fig. S7 *A* and *B*, respectively) to examine species-specificity as well as development-specificity. Then we generated a heat map hierarchical cluster of the 30 glycans that showed significant developmental changes in both seven human age groups and six mouse age groups (*SI Appendix*, Fig. S8*A*). The 13 age groups were divided into roughly four groups in dendrograms; a human younger group excluding neonates (infant, toddler, and school age), a human older group (teenager, young adult, and adult), and a mouse older group (6, 10, and 43 wk) were completely separated as three superior clusters, whereas human neonates were coclustered with a mouse younger group (1, 2, and 3 wk). Notably, these results clearly indicated that the glycosylation pattern at an early developmental stage is highly conserved between two species. In other words, development-specific traits were strongly evident in the early developmental stage regardless of species, whereas species-specific traits seemed to become more pronounced during the development process. Interestingly, we screened the developmental patterns of

glycans and found that most of the glycans that were highly expressed in an older group of both human and mouse tend to present a positive correlation with aging (highlighted with red box in *SI Appendix*, Fig. S8*A*). On the other hand, the glycans that are abundant in younger group of both human and mouse had a tendency to have a negative correlation with aging (highlighted with blue box in *SI Appendix*, Fig. S8*A*).

Quantitative changes in 30 glycans that were closely associated with PFC development in both humans and mice were assessed using box plots, as shown in *SI Appendix*, Fig. S9. Representative N-glycans showing changes during development in both the human and mouse PFC are plotted in *SI Appendix*, Fig. S8*B*. Two sialylated LacdiNAc N-glycans ($Hex_3HexNAc_6Fuc_1NeuAc_2$ and $Hex_4HexNAc_5Fuc_2NeuAc_1$) and a single N-glycan containing an HNK-1 moiety (HSO_3-$Hex_5HexNAc_5Fuc_2HexA_1$) were substantially decreased. In contrast, a glycan bearing a bisecting GlcNAc (HexNAc) containing a core fucose corresponding to $Hex_3HexNAc_4Fuc_1$ showed a constant increase during development in both species. Interestingly, these results are in agreement with previous studies showing that a compound containing bisecting GlcNAc (HexNAc) with a core fucose in rodents was increased in the developing mouse cerebral cortex (40, 41). Furthermore, glycans that differ by addition or deletion of monosaccharide residues in the compositions exhibited similar decreasing or increasing trends as follows; $Hex_5HexNAc_3Fuc_1NeuAc_1$ and $Hex_6HexNAc_3Fuc_1NeuAc_1$; $Hex_4HexNAc_5Fuc_2$ and $Hex_4HexNAc_5Fuc_2NeuAc_1$; $Hex_4HexNAc_6Fuc_1$, $Hex_4HexNAc_6Fuc_1NeuAc_1$, $Hex_4HexNAc_7Fuc_1NeuAc_1$, and $Hex_5HexNAc_7Fuc_1NeuAc_1$. These results clearly indicate that glycosylation is the consequence of a stepwise enzymatic process, not an independent synthetic event.

Structure and Bio-Synthetic Implications of the PFC N-Glycome. To understand glyco-synthesis processes in the human PFC, we further selected 23 backbone (main) glycans representing branching types consisting of only hexose and HexNAc (not in including modification and capping) of 52 glycan compositions with 100% detection frequency (occurrence) in human PFCs, regardless of age status. To construct a structure- and isomer-specific map, 37 isomer-specific glycans corresponding to 23 glycan compositions were extensively elucidated by retention time, MS/MS, and well-known glycans released from a standard glycoprotein (IgG) as described in *SI Appendix*, *Supplementary Methods*. Finally, the backbone glycan map was reconstituted by applying glyco-synthetic rules (18) to the 37 glycans, establishing the major branching pathway of human PFC N-glycosylation (Fig. 6*A*, structure-specific map using 23 glycans; *SI Appendix*, Fig. S10, compositional map of the 52 glycans). Indeed, 34 glycans depicted in the map were organically connected to each other, implying that highly heterogeneous PFC glycans follow the rules of glyco-synthesis. As depicted in the map, after formation of an HM type from a precursor, hybrid- and complex-type pathways are initiated by addition of a GlcNAc residue to $Man_5GlcNAc_2$. Then, the hybrid-type pathway proceeds through elongation (the addition of monosaccharides), whereas the complex-type pathway extends from $Man_3GlcNAc_3$. Importantly, determining the different pathways for synthesizing each glycan isoform could provide valuable insight into the molecular mechanism underlying human PFC glycome dynamics during development. Note that the map suggests specifically weighted pathways that produce hybrid and bisecting types and LacdiNAc in the brain (Fig. 6*A*, purple line), because hybrid and bisecting complex-type glycans containing four HexNAc (i.e., $Hex_3HexNAc_4$, $Hex_4HexNAc_4$, and $Hex_5HexNAc_4$) are uniquely observed in brain tissue, whereas biantennary complex types are predominantly presented in human blood glycans (42). Using the same process described above, we constructed mouse PFC N-glycosylation pathways. Interestingly, mouse PFC N-glycans appear to have an identical mainstream pathway of branching linking the 34 glycans shown in Fig. 6*A*, suggesting that the mouse could be a viable model for research on human brain development.

In addition to mapping branching pathways, we also separately considered unusual terminal glycan structures identified in our dataset, including sulfated HexHexNAc, sialylated HexNAc, (sialylated) LacdiNAc, nonsulfated HNK-1, HNK-1, and phosphorylated mannose, to further characterize PFC glycosylation synthetic processes (Fig. 6*B*). These glycans were highly expressed in the brain compared with human and mouse blood. We also observed several well-known potential epitopes, such as Lewis X (or Lewis A), sialyl Lewis X (or sialyl Lewis A), and Lewis Y (or Lewis b). Finally, we suggested a putative structure map of total 142 human PFC glycan compositions (*SI Appendix*, Fig. S11). Based on MS/MS analysis and known glycobiology, hypothetically possible structures for each composition were presented. We found that among the total glycans presented in the PFC glyco-map (*SI Appendix*, Fig. S11), modified and capped forms (i.e., sulfation, phosphorylation, fucosylation, and sialylation) of 34 glycans shown in Fig. 6*A* account for most PFC glycans, specifically corresponding to 98% and 96% of total NAPIs of entire human and mouse PFC glycans, respectively. In order to pinpoint a development-specific pathway of glyco-synthesis, 30 glycans that were significantly changed in both human and mouse are indicated by red boxes in *SI Appendix*, Fig. S11 ($P < 0.01$, ANOVA). Importantly, the glycans were sialylated and fucosylated species derived from almost all branching types, suggesting that final decorations are the key factor in PFC development rather than branching process.

Furthermore, our map showing the biological connections of brain glycans not only integrates findings for individual glycans, but also confers biological plausibility to them in the context of biosynthesis. For example, incompletely processed asialo- or asialo-agalacto structures have been reported as brain-specific structural elements in diverse species, including bovine, mouse, rat, and human (39). Our results show that many biantennary glycans were either not galactosylated at all, or were only partially galactosylated, as exemplified by $Hex_4HexNAc_4$ and $Hex_5HexNAc_4$, which were previously found to be the complex type in several cell surface proteins (43) and plasma proteins (37, 44). These results suggest that a hybrid-type synthesis trajectory is favored in the brain. In addition, brain-specific features during development are corroborated by studies on glyco-enzymes. For example, Shaper and colleagues (45), suggested that the strikingly unusual feature of galactosylation could be interpreted to reflect brain-specific expression of β-1,4-galactosyltransferase (β4Gal-T). β4Gal-T6 is expressed almost solely in the adult brain. This is in contrast to housekeeping β4Gal-T1, which is abundant in most tissue but weakly expressed in fetal and adult brain. Given our brain N-glycome profile results showing preferential sialylation of highly branched glycans, it is possible that β4Gal-T6 is specific for highly branched glycans or that brain-specific galactosidase cleaves galactose specifically in less branched glycans. In addition, Hase and colleagues (46) suggested that a unique isomer structure of $Hex_3HexNAc_4Fuc_1$ bearing bisecting GlcNAc and core fucose without GlcNAc on the (α1–3) mannose branch might be generated by hexosaminidase B, which hydrolyzes the terminal GlcNAc residue in $Hex_3HexNAc_5Fuc_1$ (Fig. 6*A*, yellow line).

Discussion

The importance of glycosylation in the brain has increasingly become apparent as biological evidence accumulates demonstrating the link between glycosylation and neuroscience. However, there has been no comprehensive study of alterations in glycosylation with mammalian brain regions and development. Here, we performed large-scale N-glycan profiling of the mammalian brain at different brain regions and ages to determine the spatial and temporal diversity of glycosylation.

Most of our current understanding of brain glycosylation comes from studies on rodents because of the relative unavailability of

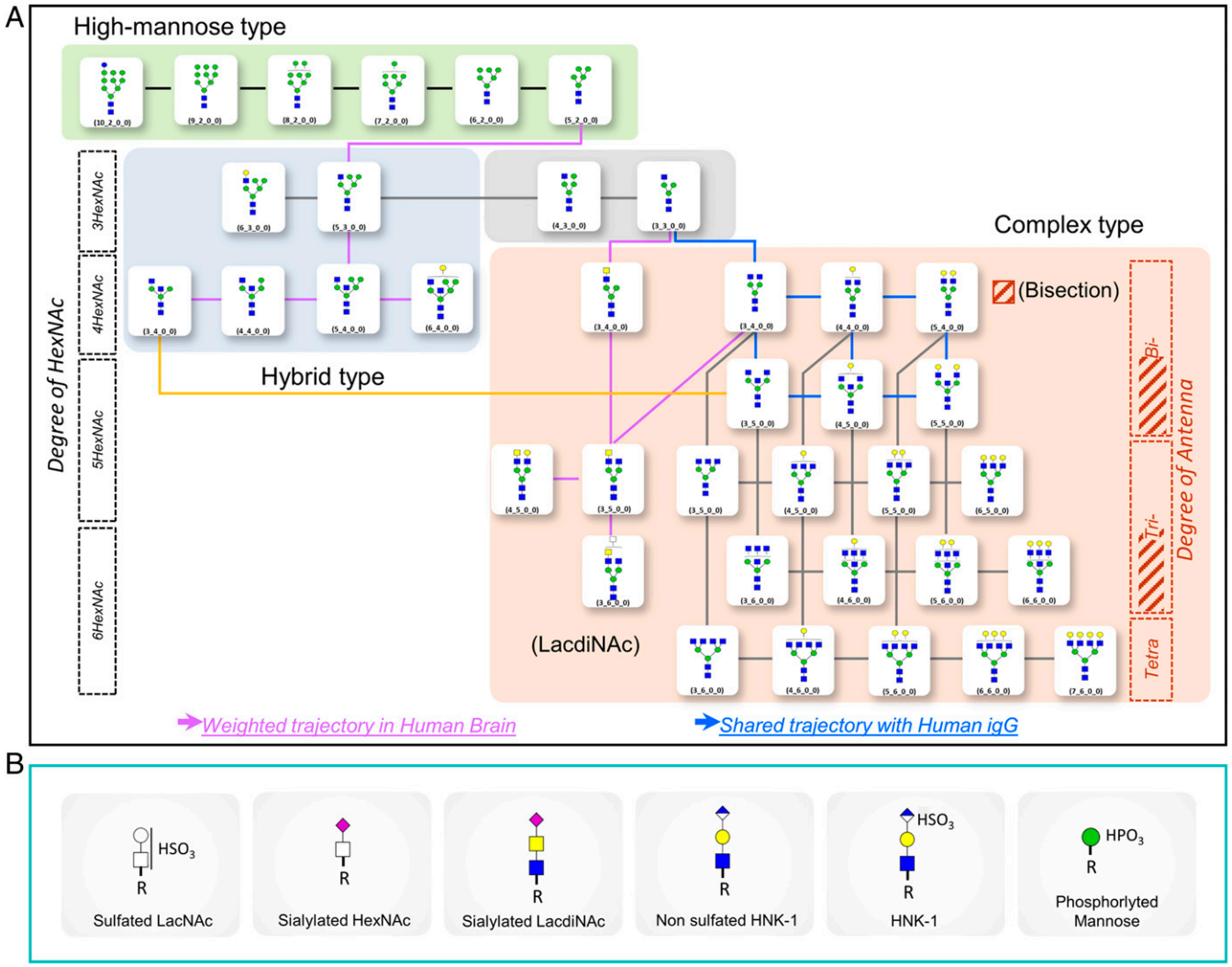

Fig. 6. Model of human PFC N-glycan synthesis. (*A*) Proposed branching pathway of major N-glycans in the human and mouse PFC. Modification and capping by fucose and sialic acid are not presented. Glycan schematic symbols: yellow circle, galactose; blue circle, glucose; green circle, mannose; blue square, N-acetyl glucosamine; red triangle, fucose; purple diamond, NeuAc; and light gray diamond, NeuGc. (*B*) Distinctive terminal glycan structures found in human and mouse PFCs.

human samples and inadequacy of analytical methods. There have been reports of highly conserved "brain-type" glycans in different mammalian species, but few studies have been done on the similarities and differences between humans and mice, particularly in terms of glycosylation in the brain (39). We elucidated interspecies similarities in brain glycosylation in humans and mice as well as intraspecies differences in glycosylation between serum and brains. In particular, we found significantly higher interspecies similarities in glycosylation in the brain than in the blood because of the suppression of NeuGc modifications in the mouse brain. In this context, Varki and colleagues (47) suggested that evolutionary selection for sustained inhibition of NeuGc expression may reflect negative effects of NeuGc on neural development or function. Our results demonstrate the usefulness of the mouse as a valuable animal model for ultimately understanding human brain glycosylation.

Interestingly, region-specific and age-specific glycans with unique structural features, such as LacdiNAc and HNK-1 epitopes, as well as brain-specific glycans including well known bisecting types, were characterized in both the human and mouse brain using our sensitive analytical techniques. Additional analyses are definitely required to identify specific linkages of unusual glycans. Nonetheless, the changes in N-glycosylation patterns in our dataset strongly suggest that N-glycans play important roles in mammalian brain region-specificity and brain development. Our findings suggest a global biosynthetic picture of glycosylation in the PFC. Based on the core N-glycans presented in the glycomap, the overall diversity of PFC N-glycosylation could be extended by considering the capping and modifications of glycans. Indeed, capped and modified versions of core glycans in the map account for 87% qualitatively and 98% quantitatively (NAPI) of all human PFC glycans. However, construction of a comprehensive isomer- and structure-specific map connecting all individual glycans observed in the brain has been hampered by current methodological limitations, such as the lack of glycan standards, endogenous exo- and endo-glycosidase activities, and low sample amounts. Nonetheless, our findings suggest a weighted synthetic trajectory of brain glycans that is distinct from that of the blood, pointing to the need for an in-depth structure-specific examination of brain glycosylation to expand our knowledge of relationships between glycan structures and brain functions.

Together, there is no doubt that our comprehensive profile of glycosylation patterns in human and mouse brains represents a valuable reference for future mammalian brain glycome studies. Several postmortem studies in human have previously shown that glycan biosynthesis or levels of glycan were changed in the specific protein from PFC areas of patients with a psychiatric disorder, such as schizophrenia (48–50). On a broader perspective, our current findings and methodologies may assist in future studies that seek to examine the causality of altered glycome in the PFC-related cognitive or emotional functions as well as the PFC regarding pathogenesis of psychiatric diseases.

Materials and Methods

Details of the experimental protocols can be found in *SI Appendix, Supplementary Methods*.

Human and Mouse Brain Tissue Collection. Postmortem tissues from the dorsolateral PFC (Brodmann Area 46) of 68 individuals ranging in age from 6 wk to 49 y were obtained from the National Child Health and Human Development Brain and Tissue Bank for Developmental Disorders at the University of Maryland, Baltimore, MD. All procedures for preparation of mouse brain dissections were performed in compliance with the Institute for Basic Science Institutional Animal Care and Use Committee guidelines.

Sample Preparation for LC-MS. Membranes containing various glycoproteins were selectively extracted from dissected brain tissues using ultracentrifugation. Membrane protein-bound N-glycans were subsequently enzymatically released by treating with PNGase F and enriched by PGC solid-phase extraction (22).

LC-MS and Collision-Induced Dissociation and MS/MS Analyses of Brain N-Glycans. Chromatographic separation and structure-specific profiling of brain N-glycans was accomplished by MS analysis performed on an Agilent 6530 Q-TOF mass spectrometer coupled to an Agilent 1260 series LC system (Agilent Technologies).

LC-MS Data Analysis and Glycan Identification. Glycans were initially determined by accurate masses, retention times, and known glycan biosynthetic correlations (18, 47) and their putative structures were further elucidated by collision-induced dissociation and MS/MS. The abundance of each N-glycan composition was normalized to total ion counts.

Statistical Analysis. Sample profiles were then compared by statistically evaluating NAPI values using sPLS networks (51), sPLS-DA, and ANOVA.

Data Availability. All study data are included in the article and *SI Appendix* .

ACKNOWLEDGMENTS. This work was supported by the Institute for Basic Science (IBS-R001-D1-2019-a00) and the National Research Council of Science and Technology (CAP-15-03-KRIBB). C.S.W. is funded by the New South Wales Ministry of Health, Office of Health and Medical Research. C.S.W. is a recipient of a National Health and Medical Research Council (Australia) Principal Research Fellowship (1117079).

1. M. J. Hawrylycz *et al.*, An anatomically comprehensive atlas of the adult human brain transcriptome. *Nature* **489**, 391–399 (2012).
2. J. Ivanisevic *et al.*, Brain region mapping using global metabolomics. *Chem. Biol.* **21**, 1575–1584 (2014).
3. L. Ng *et al.*, An anatomic gene expression atlas of the adult mouse brain. *Nat. Neurosci.* **12**, 356–362 (2009).
4. K. Sharma *et al.*, Cell type- and brain region-resolved mouse brain proteome. *Nat. Neurosci.* **18**, 1819–1831 (2015).
5. E. S. Lein *et al.*, Genome-wide atlas of gene expression in the adult mouse brain. *Nature* **445**, 168–176 (2007).
6. T. E. Bakken *et al.*, A comprehensive transcriptional map of primate brain development. *Nature* **535**, 367–375 (2016).
7. C. K. Frese *et al.*, Quantitative map of proteome dynamics during neuronal differentiation. *Cell Rep.* **18**, 1527–1542 (2017).
8. M. Jové, M. Portero-Otín, A. Naudí, I. Ferrer, R. Pamplona, Metabolomics of human brain aging and age-related neurodegenerative diseases. *J. Neuropathol. Exp. Neurol.* **73**, 640–657 (2014).
9. K. Ohtsubo, J. D. Marth, Glycosylation in cellular mechanisms of health and disease. *Cell* **126**, 855–867 (2006).
10. R. K. Margolis, R. U. Margolis, "Structure and distribution of glycoproteins and glycosaminoglycans" in *Complex Carbohydrates of Nervous Tissue*, R. U. Margolis, Ed. (Springer, 1979), pp. 45–73.
11. N. Yamakawa *et al.*, Systems glycomics of adult zebrafish identifies organ-specific sialylation and glycosylation patterns. *Nat. Commun.* **9**, 4647 (2018).
12. R. Kleene, M. Schachner, Glycans and neural cell interactions. *Nat. Rev. Neurosci.* **5**, 195–208 (2004).
13. S. Hakomori, Glycosphingolipids in cellular interaction, differentiation, and oncogenesis. *Annu. Rev. Biochem.* **50**, 733–764 (1981).
14. K. S. Lau *et al.*, Complex N-glycan number and degree of branching cooperate to regulate cell proliferation and differentiation. *Cell* **129**, 123–134 (2007).
15. V. Zoldoš, T. Horvat, G. Lauc, Glycomics meets genomics, epigenomics and other high throughput omics for system biology studies. *Curr. Opin. Chem. Biol.* **17**, 34–40 (2013).
16. National Research Council, *Transforming Glycoscience: A Roadmap for the Future* (National Academies Press, 2012).
17. D. F. Zielinska, F. Gnad, K. Schropp, J. R. Wiśniewski, M. Mann, Mapping N-glycosylation sites across seven evolutionarily distant species reveals a divergent substrate proteome despite a common core machinery. *Mol. Cell* **46**, 542–548 (2012).
18. R. Cummings, F. Liu, G. Vasta, "Chapter 1: Historical Background and Overview" in *Essentials of Glycobiology*, A. Varki, Ed. (Cold Spring Harbor Laboratory Press, Cold Spring Harbor, NY, 3rd Ed., 2017).
19. P. M. Rudd, A. H. Merry, M. R. Wormald, R. A. Dwek, Glycosylation and prion protein. *Curr. Opin. Struct. Biol.* **12**, 578–586 (2002).
20. W.-N. Gao *et al.*, Microfluidic chip-LC/MS-based glycomic analysis revealed distinct N-glycan profile of rat serum. *Sci. Rep.* **5**, 12844 (2015).
21. D. Wu, W. B. Struwe, D. J. Harvey, M. A. Ferguson, C. V. Robinson, N-glycan microheterogeneity regulates interactions of plasma proteins. *Proc. Natl. Acad. Sci. U.S.A.* **115**, 8763–8768 (2018).
22. I. J. Ji *et al.*, Spatially-resolved exploration of the mouse brain glycome by tissue glycocapture (TGC) and nano-LC/MS. *Anal. Chem.* **87**, 2869–2877 (2015).
23. A. Diamond, "Normal development of prefrontal cortex from birth to young adulthood: Cognitive functions, anatomy, and biochemistry" in *Principles of Frontal Lobe Function*, D. T. Stuss, R. T. Knight, Eds. (Oxford University Press, New York, 2002), pp. 466–503.
24. J. M. Fuster, Frontal lobe and cognitive development. *J. Neurocytol.* **31**, 373–385 (2002).
25. B. D. Semple, K. Blomgren, K. Gimlin, D. M. Ferriero, L. J. Noble-Haeusslein, Brain development in rodents and humans: Identifying benchmarks of maturation and vulnerability to injury across species. *Prog. Neurobiol.* **106**, 1–16 (2013).
26. M. Gotoh *et al.*, Molecular cloning and characterization of β1,4-N-acetylgalactosaminyltransferases IV synthesizing N,N′-diacetyllactosediamine. *FEBS Lett.* **562**, 134–140 (2004).
27. E. Machado *et al.*, N-Glycosylation of total cellular glycoproteins from the human ovarian carcinoma SKOV3 cell line and of recombinantly expressed human erythropoietin. *Glycobiology* **21**, 376–386 (2011).
28. K. Fukushima, T. Satoh, S. Baba, K. Yamashita, α1,2-Fucosylated and β-N-acetylgalactosaminylated prostate-specific antigen as an efficient marker of prostatic cancer. *Glycobiology* **20**, 452–460 (2010).
29. D. Fiete, V. Srivastava, O. Hindsgaul, J. U. Baenziger, A hepatic reticuloendothelial cell receptor specific for SO4-4GalNAc β 1,4GlcNAc β 1,2Man α that mediates rapid clearance of lutropin. *Cell* **67**, 1103–1110 (1991).
30. N. Sasaki, M. Shinomi, K. Hirano, K. Ui-Tei, S. Nishihara, LacdiNAc (GalNAcβ1-4GlcNAc) contributes to self-renewal of mouse embryonic stem cells by regulating leukemia inhibitory factor/STAT3 signaling. *Stem Cells* **29**, 641–650 (2011).
31. T. Sato, J. Taka, N. Aoki, T. Matsuda, K. Furukawa, Expression of β-N-acetylgalactosaminylated N-linked sugar chains is associated with functional differentiation of bovine mammary gland. *J. Biochem.* **122**, 1068–1073 (1997).
32. T. Torii *et al.*, Determination of major sialylated N-glycans and identification of branched sialylated N-glycans that dynamically change their content during development in the mouse cerebral cortex. *Glycoconj. J.* **31**, 671–683 (2014).
33. A. K. Saghatelyan *et al.*, The extracellular matrix molecule tenascin-R and its HNK-1 carbohydrate modulate perisomatic inhibition and long-term potentiation in the CA1 region of the hippocampus. *Eur. J. Neurosci.* **12**, 3331–3342 (2000).
34. D. K. Chou, J. E. Evans, F. B. Jungalwala, Identity of nuclear high-mobility-group protein, HMG-1, and sulfoglucuronyl carbohydrate-binding protein, SBP-1, in brain. *J. Neurochem.* **77**, 120–131 (2001).
35. S. Yamamoto *et al.*, Mice deficient in nervous system-specific carbohydrate epitope HNK-1 exhibit impaired synaptic plasticity and spatial learning. *J. Biol. Chem.* **277**, 27227–27231 (2002).
36. J. C. Izpisua Belmonte *et al.*, Brains, genes, and primates. *Neuron* **86**, 617–631 (2015).
37. S. Hua *et al.*, Isomer-specific LC/MS and LC/MS/MS profiling of the mouse serum N-glycome revealing a number of novel sialylated N-glycans. *Anal. Chem.* **85**, 4636–4643 (2013).
38. L. R. Davies, A. Varki, "Why is N-glycolylneuraminic acid rare in the vertebrate brain?" in *SialoGlyco Chemistry and Biology I*, R. Gerardy-Schahan, P. Delannoy, M. von Itzstein, Eds. (Springer, 2013), pp. 31–54.
39. C. Albach, R. A. Klein, B. Schmitz, Do rodent and human brains have different N-glycosylation patterns? *Biol. Chem.* **382**, 187–194 (2001).

40. A. Ishii *et al*., Developmental changes in the expression of glycogenes and the content of N-glycans in the mouse cerebral cortex. *Glycobiology* **17**, 261–276 (2007).
41. S. Nakakita, S. Natsuka, K. Ikenaka, S. Hase, Development-dependent expression of complex-type sugar chains specific to mouse brain. *J. Biochem.* **123**, 1164–1168 (1998).
42. S. R. Kronewitter *et al*., The development of retrosynthetic glycan libraries to profile and classify the human serum N-linked glycome. *Proteomics* **9**, 2986–2994 (2009).
43. D. Chui *et al*., Alpha-mannosidase-II deficiency results in dyserythropoiesis and unveils an alternate pathway in oligosaccharide biosynthesis. *Cell* **90**, 157–167 (1997).
44. J. Lee *et al*., Designation of fingerprint glycopeptides for targeted glycoproteomic analysis of serum haptoglobin: Insights into gastric cancer biomarker discovery. *Anal. Bioanal. Chem.* **410**, 1617–1629 (2018).
45. N.-W. Lo, J. H. Shaper, J. Pevsner, N. L. Shaper, The expanding β4-galactosyltransferase gene family: Messages from the databanks. *Glycobiology* **8**, 517–526 (1998).
46. Y. Okamoto, K. Omichi, S. Yamanaka, K. Ikenaka, S. Hase, Conversion of brain-specific complex type sugar chains by N-acetyl-β-D-hexosaminidase B. *J. Biochem.* **125**, 537–540 (1999).
47. Y. Naito-Matsui *et al*., Physiological exploration of the long term evolutionary selection against expression of *N*-glycolylneuraminic acid in the brain. *J. Biol. Chem.* **292**, 2557–2570 (2017).
48. D. Bauer, V. Haroutunian, J. H. Meador-Woodruff, R. E. McCullumsmith, Abnormal glycosylation of EAAT1 and EAAT2 in prefrontal cortex of elderly patients with schizophrenia. *Schizophr Res.* **117**, 92–98 (2010).
49. J. Tucholski *et al*., Abnormal N-linked glycosylation of cortical AMPA receptor subunits in schizophrenia. *Schizophr Res.* **146**, 177–183 (2013).
50. T. M. Mueller, V. Haroutunian, J. H. Meador-Woodruff, N-glycosylation of GABA A receptor subunits is altered in schizophrenia. *Neuropsychopharmacology* **39**, 528–537 (2014).
51. J. Bartel, J. Krumsiek, F. J. Theis, Statistical methods for the analysis of high-throughput metabolomics data. *Comput. Struct. Biotechnol. J.* **4**, e201301009 (2013).